



HAL
open science

Operando Infrared (IR) Coupled to SSITKA for Photocatalysis: Reactivity and Mechanistic Studies

Mohamad El-Roz, Philippe Bazin, Marco Daturi, Frederic Thibault-Starzyk

► **To cite this version:**

Mohamad El-Roz, Philippe Bazin, Marco Daturi, Frederic Thibault-Starzyk. Operando Infrared (IR) Coupled to SSITKA for Photocatalysis: Reactivity and Mechanistic Studies. *ACS Catalysis*, 2013, 3 (12), pp.2790-2798. hal-01963787

HAL Id: hal-01963787

<https://hal.science/hal-01963787v1>

Submitted on 5 Oct 2021

HAL is a multi-disciplinary open access archive for the deposit and dissemination of scientific research documents, whether they are published or not. The documents may come from teaching and research institutions in France or abroad, or from public or private research centers.

L'archive ouverte pluridisciplinaire **HAL**, est destinée au dépôt et à la diffusion de documents scientifiques de niveau recherche, publiés ou non, émanant des établissements d'enseignement et de recherche français ou étrangers, des laboratoires publics ou privés.

***Operando* IR coupled to SSITKA for photocatalysis: reactivity and mechanistic studies.**

Mohamad El-Roz*, Philippe Bazin, Marco Daturi, Frederic Thibault-Starzyk

Laboratoire Catalyse et Spectrochimie, ENSICAEN, Université de Caen, CNRS, 6, boulevard du Maréchal Juin, 14050 Caen, France.

**email: mohamad.elroz@ensicaen.fr*

Abstract

This paper reports the coupling of *operando* IR and SSITKA (Steady State Isotopic Transient Kinetic Analysis) for air purification studies from VOCs by photocatalysis. Methanol photooxidation has been used as a model reaction. A new photocatalyst (TiO₂-L) has been studied and compared to the reference material TiO₂-P25. The TOF and reaction rate have been calculated and compared. We show that TOF values are not really available in heterogeneous photocatalysis where the number of active sites can vary from one TiO₂ material to the other and from one experimental setup to the other. The influence of methanol concentration and reaction temperature on photocatalytic activity and on selectivity was also investigated. TiO₂-L is more active than TiO₂-P25 at low methanol concentration and more selective at high methanol concentrations. SSITKA clarified the role of the surface formate species in the reaction mechanism. Most of these formate species are spectators and are not the main intermediates in alcohol photooxidation. A graduation was found in the efficiency of active sites on photocatalyst surfaces.

Keywords: IR-*operando*, SSITKA, photocatalysis, TiO₂, methanol photooxidation, methyl formate, CO₂-selectivity, air purification.

1. Introduction

The exponential growth of population accompanied with a high increase of industrial and military activities have caused a rapid degradation of air and water quality in the last few years. Consequently, environmental pollution is now a major global priority, requiring a considerable research effort. New analytical, biochemical, and physicochemical methods are

developed and studied for the characterization and elimination of hazardous chemical compounds from air, soil, and water. Advanced oxidation processes (AOPs), and especially heterogeneous photocatalysis, are intended to be both supplementary and complementary to some of the more conventional approaches to the destruction and/or transformation of hazardous chemical wastes such as filtration¹, anaerobic digestion², and conventional physicochemical treatment³⁻⁶. In the field of air cleaning technologies, heterogeneous photocatalysis is a well established and widely investigated process for the oxidation of many pollutants in air, especially indoor air where pollution can be even more important.^{7,8} More than 2000 companies now commercialize different photocatalytic products, mainly for self-cleaning applications.⁷⁻⁹ Therefore, the developments of new techniques and methods to investigate photocatalytic activity of solids, in water and/or air, become more and more important. During the last decade, more than 22 10³ papers on photocatalysis have been published, out of which only ~5% deal with its application to air purification versus more than 32% for water purification.^{10,11} The reasons for this could well be experimental difficulties, since studying heterogeneous photocatalysis is often more difficult in the gas phase than in the liquid phase:

- (i) contrarily to water purification where the photocatalyst can be used as a suspension, photocatalysis processes (or studies) for air purification require the fixation of the photocatalyst on a support or/and on the reactor surface. This needs, in most cases, the use of a binder, which could influence photocatalytic activity;
- (ii) a homogenous and reproducible irradiation of the photocatalyst surfaces is needed in order to have reproducible experiments and results;
- (iii) the amount of photocatalyst used must be known accurately and the loss of material during the reaction must be kept to a minimum;
- (iv) for spectroscopic studies, the design of the reactor can be difficult, and, for example, the internal volume of the reactor must be kept as small as possible to minimize the optical pathway in the gas phase and to decrease residence time;
- (v) the reaction parameters (e.g. air composition, air flow (or contact time), temperature, irradiation intensity...) must be easily and accurately controlled, etc...

For these reasons, we have developed recently a new *operando* IR reactor for studying photocatalytic processes for air purification.^{12,13} This technique presents several advantages:

- (i) the photocatalyst is used and studied under the form of thin pellets, which allows limiting

the mass loss, with an accurate control of the photocatalyst mass, and which ensures a homogenous irradiation of the photocatalyst surface;

(ii) the irradiation intensity can be easily controlled and the irradiation source can be changed (to mono or polychromatic irradiations, UV and/or visible light sources...) without changing the photoreactor;

(iii) the dead volume is reduced to about 0.4 ml (residual space between each sample face and the photoreactor windows);

(iv) the reactor is coupled to on line analysis techniques, such as IR gas cell and mass spectroscopy (or GC-MS), which provides photocatalytic activity and selectivity data with high precision;

(v) the heating temperature of the reactor-cell can be controlled from RT to 600°C, and the VOCs (volatile organic compounds) or different gas concentrations from a few ppm to a few %. The air composition (VOCs mixture, humidity, toxic gas...) and the gas flow (from 1 to 50 cm³/min) can reproduce the real conditions of the photocatalytic reaction and the influence of these parameters on photocatalytic activities and selectivities is easily studied.

This paper demonstrates the reliability of this technique in the study of the photoactivity and selectivity of a newly elaborated TiO₂ photocatalyst (TiO₂-L) and of TiO₂-P25 (Evonik-Degussa) in the purification of air from methanol used as a model molecule for VOCs. We already presented previously the role of surface sites for the adsorption of reactants and for the formation of intermediates in room temperature methanol photooxidation¹². The usually accepted mechanism involves formate species as main intermediates (as is the case for thermal oxidation¹⁴), since these formates were detected by IR spectroscopy on the surface, but no kinetic proof for the validation of this hypothesis has ever been reported.^{12,15,16} For these reasons, we further investigated this system using the SSITKA approach (isotopic exchange techniques (¹²CH₃OH/¹³CH₃OH)) combined with infrared (IR) *operando* analysis system, a methodology which has already shown excellent results in methanol oxidation studies¹⁷ but was up to now not accessible in photocatalysis. We also report the influence of some other parameters on the CO₂-selectivity and activity of TiO₂, like the temperature and the methanol concentration of.

2. Experimental section

2.1. Synthesis and characterization of TiO₂-L

Hierarchical TiO₂ (TiO₂-L) has been synthesized and characterized as described in reference [18]. The seeding of natural Luffa sponge (used as biotemplate) with TiO₂ anatase was accomplished by a 24 h hydrothermal synthesis at 100°C, under autogeneous pressure. A synthesis mixture with the following composition 10Ti(OEt)₄:45C₂H₅OH:45H₂O (vol.%) was used. The precursor solution was stirred with the Luffa sponges at room temperature for 1 h. Then, 100 ml of the solution (together with 500 mg of Luffa sponge) was poured into Teflon-lined stainless steel autoclaves. After the synthesis, the Luffa sponges were removed from the autoclaves, thoroughly cleaned (in order to remove the excess of TiO₂ seeds loosely bound on the substrate) with ethanol and water, and dried overnight at 60°C. After rinsing, the samples (TiO₂/Luffa) were calcined under air: 5 h ramp to 500°C and 5 h dwell time. A macro-tubular TiO₂ shape with macro-channel was obtained after removal of the natural organic support (replica of luffa fibers) (Figure S-1). Then, TiO₂-L samples were characterized using XRD, N₂ sorption and UV-vis spectroscopy;¹⁸ the results are collected in Table 1. As a comparison, the photooxidation was also performed on a commercial TiO₂ from Evonik-Degussa (TiO₂-P25).

2.2. Photocatalysis

The photocatalytic oxidation of methanol was performed using the new *operando* IR reactor described in reference [13]. The TiO₂-L and TiO₂-P25 (Degussa) were pressed into self-supported wafers ($\varnothing = 16$ mm, $m = \sim 10$ mg/cm²; thickness = 50-60 μ m (measured by Micromaster-IP54)). The cell was connected to gas lines with gas mixing devices and mass flow controllers. The two gas mixtures, so called activation and reaction flows, could be prepared and sent independently to the reactor cell. Exhaust gases (reactive and/or reaction products) can be analyzed by a Quadrupole Mass Spectrometer (Pfeiffer Omnistar GSD 301), while complementary information on the gas phase can be gained by IR spectroscopy through a gas micro-cell. IR spectra (64 scans per spectrum) of the catalyst under working conditions were collected at a time resolution of 1 spectrum each 2 minutes with a Thermo Scientific Nicolet 6700 spectrometer, equipped with a MCT detector. More details can be found in the following references for both the *operando* IR system [19-21] and the modified IR reactor-

cell [12]. All IR spectra are displayed as absorbance. For this specific study, the system was equipped with two saturators in the same thermostatic bath (at exactly the same temperature), in order to send, via a 4 ways valve, a fixed concentration of vaporized methanol, either in its natural form or 99.0% ^{13}C enriched, provided by Cambridge Isotope Laboratories. The flow conditions were as follows: 400-1200 ppm CH_3OH , 20% oxygen in Argon at $60,000\text{ h}^{-1}$ constant gas hourly space velocity. A calibration curve was drawn to establish the linear relationship between the concentration of methanol and the MS (at $m/z=29$) and IR (at $1038\text{-}1026\text{ cm}^{-1}$) signals (Figure S-1). The reaction was studied at RT. A monochromatic UV irradiation at 365 nm with $I_0\sim 11\text{ mW/cm}^2$ was used in order to simplify the discussion of the results. It was applied with a Xe-Hg lamp (LC8 Spot Light Hamamatsu, L10852, 200 W) and a 365 nm band pass filter (Hamamatsu). A UV-light guide (A10014-50-0110) mounted at the entrance of a modified operando IR cell was used to establish a homogeneous irradiation, (as shown in Scheme S1 in supplementary information). N.B.: under polychromatic irradiation (reference 13), TiO_2 presents a higher activity and selectivity than here under monochromatic irradiation. Under the same irradiation conditions, $\text{TiO}_2\text{-25}$ presented the same activity here as in our previous work. The methanol conversion and CO_2 -selectivity were calculated as reported in our previous work.¹²

3. Results and discussion

3.1 photocatalytic activity and selectivity of $\text{TiO}_2\text{-L}$ and $\text{TiO}_2\text{-P25}$ and effect of the methanol concentration

In order to compare photocatalytic activity and selectivity for $\text{TiO}_2\text{-L}$ and $\text{TiO}_2\text{-P25}$, the photooxidation of methanol was performed under the same conditions for different methanol concentrations ($[\text{MeOH}]$). The concentration of methanol in the gas was measured using the surface area of the MeOH-IR band at $1090\text{-}950\text{ cm}^{-1}$ and the MeOH-MS signal at $m/z=29$ (a calibration curve is presented in Figure S-2). Selectivity for CO_2 (selectivity of the reaction for a complete methanol mineralization) was determined using the IR band area at $2395\text{-}2182\text{ cm}^{-1}$ and/or the MS signal at $m/z=44$. Figure 1 presents the evolution of methanol conversion and CO_2 -selectivity versus MeOH concentration. For each concentration, methanol conversion and CO_2 -selectivity were calculated after the stabilization of the gas phase IR spectra and MS signals, i.e. 30min to 1h irradiation time after each flow modification (Figure S-3). As reported in our previous work,¹³ the methanol concentration can influence

significantly the activity and the selectivity of the reaction. For a concentration lower than 600 ppm, TiO₂-L shows a higher activity and similar CO₂-selectivity than TiO₂-P25 (Figure 1). In this range of concentration, the CO₂-selectivity is slightly affected for both TiO₂-L and TiO₂-P25. For a concentration higher than 600 ppm, the methanol conversion on TiO₂-L is lower than on TiO₂-P25. An important decrease in the CO₂-selectivity could be also observed, less pronounced on TiO₂-L than on TiO₂-P25. New IR bands at 1755 cm⁻¹ and 1890 cm⁻¹, assigned respectively to $\nu(\text{C}=\text{O})$ and $\nu(\text{C}-\text{O})$ vibration modes of methyl formate¹² are observed in the reaction gas phase (Figure 2). The increase of these bands (and the $m/z=60$ MS signal) with methanol concentration explains the decrease of CO₂-selectivity. The maximum amount of converted methanol (Table S1 in supplementary information) is about 700 ppm/min (with ~55% CO₂-selectivity) for TiO₂-L and about 800 ppm/min for TiO₂-P25 (with 50% CO₂-selectivity). Therefore, the maximum amount of “mineralized” methanol on both TiO₂-L and TiO₂-P25 is about 400 ppm/min (under the experiment conditions described in the experimental part). These results show that the increase in methanol concentration promotes the formation of methylformate by increasing surface coverage by methanol.

The turnover frequency (TOF) is important for comparing heterogeneous catalysts.²² As in enzymatic or homogeneous catalysis, the turnover frequency corresponds to the number of molecules converted per second and per active site (or per catalytic molecule).²³ In heterogeneous catalysis, TOF is often more difficult to determine and the number of active sites can be largely unknown and it is generally overestimated, considering all the theoretically calculated sites on the sample as accessible and active. In the case of solid/gas photocatalysis it could be even worse: the actual operating surface is not known since some parts of photocatalyst particles are not illuminated (inhomogeneous irradiation) as a consequence of internal shading.^{22,24,25} In our case, the use of the photocatalyst under the form of a thin pellet (~40 μm) allows a homogenous, reproducible and total illumination of the photocatalyst. On the other hand, the possibility of internal shading of the TiO₂ particles does not preclude the comparison between two photocatalysts where the effect will be same. Consequently, a more reliable estimation of the TOF will be used in this study for an additional comparison of TiO₂-L and TiO₂-P25. Practically, we used the surface density of titanol groups Ti-OH (equal to 5×10^{18} OH/m² or 5 OH/nm²,²⁶) as the upper limit for the number of active sites n_{sites} . The methanol conversion rate (V_{MeOH}) corresponds to the amount of methanol converted (in ml) per gram of photocatalyst ($\text{g}_{\text{cat}}^{-1}$) per minute of irradiation time

(min^{-1}). The results for TOF and V_{MeOH} are presented in Figure 3 and Table S-1. Conversion rates are similar for both photocatalysts, but since $\text{TiO}_2\text{-L}$ has a higher specific surface area (Table 1), the TOF for $\text{TiO}_2\text{-L}$ is 2 to 3 times lower than for $\text{TiO}_2\text{-P25}$. This means that the active sites are less efficient on $\text{TiO}_2\text{-L}$ than on $\text{TiO}_2\text{-P25}$ or that only a fraction of the sites are accessible or active. In the last case, the use of the theoretically estimated number of active sites is not acceptable.

Operando IR in the photocatalytic reactor shed some more light on these reactions. During UV irradiation, new bands appeared (Figures 4 and S-4), assigned to mono and bidentate formate species adsorbed on the catalyst surface.^{12,13,27,28} These species are commonly described as intermediates in the photooxidation of alcohols.^{12,15,16,29-34} We observed different vibration bands for bidentate formates on $\text{TiO}_2\text{-L}$ (maxima at 1600, 1373 and 1356 cm^{-1}) and on $\text{TiO}_2\text{-P25}$ (maxima at 1570, 1379, 1362 cm^{-1}), probably because of a difference in the nature of the formation/adsorption site. In addition, the IR intensity of these bands is much higher on $\text{TiO}_2\text{-L}$ than on $\text{TiO}_2\text{-P25}$ (Figure 4). This could be due to (i) the higher specific surface of $\text{TiO}_2\text{-L}$ (~1.6 times higher than $\text{TiO}_2\text{-P25}$) leading to a higher formation of formate species and/or to (ii) a stronger adsorption of bidentate formate species on $\text{TiO}_2\text{-L}$ than on $\text{TiO}_2\text{-P25}$, thus reducing their transformation.

The increase of methanol concentration led to a simultaneous increase of some corresponding IR band intensities, more important on $\text{TiO}_2\text{-L}$ than on $\text{TiO}_2\text{-P25}$, with a maximum at 800 ppm (Figure 5A and 5B). The same catalytic activities were observed on both photocatalysts when working in reverse concentration order, from higher to lower MeOH concentrations, which rules out surface deactivation at high methanol concentration.

These results raise the question about the alleged role of intermediates for the formates on TiO_2 surface.

3.2 Influence of temperature on the activity of $\text{TiO}_2\text{-L}$

The influence of temperature on the activity of $\text{TiO}_2\text{-P25}$ has already been discussed (under polychromatic irradiation) in a previous work¹². Results for $\text{TiO}_2\text{-L}$ are reported in Figure 6. Both activity and selectivity increase with temperature, like on $\text{TiO}_2\text{-P25}$.¹² For $T > 75^\circ\text{C}$, methanol conversion is higher than 90% (vs. ~55% at RT), with complete mineralization (vs. 60% CO_2 -selectivity at RT). Following the formate species on $\text{TiO}_2\text{-L}$ with temperature is easy due to the high intensity of the corresponding IR bands (Figure 7). An important decrease is observed with increasing temperature, with a maximum between 75°C and 100°C .

This apparent decrease of surface formates with increasing temperature (and activity) already raises the question about the role of the formates in the photocatalytic oxidation of methanol (and alcohols) and of their true intermediate nature. In addition, stationary IR bands could also be observed even at high temperature, showing the formation and presence of stable species on the photocatalyst during photooxidation.

3.3 Role of formate species in methanol photooxidation: a complementary study by SSITKA

SSITKA is a methodology for obtaining transient conditions while remaining under the required chemical and/or kinetic steady state environment for a given reaction. It is already used in some operando studies for a better understanding or for clarifying the mechanism of a catalytic reaction, and sometimes to determine the activation energy.³⁵⁻³⁹ In our case, SSITKA experiments were performed to clarify the role of formate species in methanol photooxidation. Two reaction flows in our operando system have been used, each of them equipped with a saturator containing either natural or ¹³C enriched methanol (Scheme S1). A four ways valve allows instantaneous switching from one flow to the other under the same experimental conditions (flow: 25 cm³/min, concentration: 1200 ppm, temperature: RT, UV irradiation intensity: I₀₍₃₆₆₎ ~11 mW/cm²; λ = 366 nm and air composition: 20% oxygen in Ar), and the reaction remains chemically identical in both cases. The chosen methanol concentration led to incomplete conversion and partial mineralization of methanol (Figure 1), which allowed following the isotopic exchange of all species including reactants with the on-line gas analyses. The switch from ¹²C to ¹³C-substituted methanol was done during the photooxidation reaction and the switching time was used as t = 0. The results presented here were obtained on TiO₂-P25, and those with TiO₂-L are presented in supplementary information.

Starting from the chemical steady state (t = 0), the reaction flow was switched from natural to labeled methanol. Consequently, the bands of adsorbed ¹³C-methoxy (1090 cm⁻¹) and ¹³C-formates (1340 and 1515 cm⁻¹) species progressively replaced those of the unlabeled species (Figure 8AI), giving rise to several isosbestic points. On the time traces (Figure 9A), crossing points are observed at t ~5 min and t ~18 min (> 75min for TiO₂-L; Figure S-5) for adsorbed methoxy and formate species respectively. The on-line analyses of the exhaust gases show similar isosbestic and crossing points (at t~3.7) for methanol, carbon dioxide and carbonyl compounds (methyl formate with trace of formaldehyde and/or formic acid) (Figures

8B-I, 9B, S-5). Similar results were obtained on TiO₂-L (Figure S-4). The kinetic behavior of surface methoxy groups is coherent with the kinetics of the changes in the reactor exhaust, but formate species are clearly reacting too slowly compared to the speed of CO₂ and methyl formate productions. These results show that the majority of formate species, formed on the TiO₂ surface, are spectators. This conclusion is in agreement with the relatively lower activity founded on TiO₂-L, at high methanol concentration, despite the higher amount of formate species observed on the surface of this material (compared to TiO₂-P25). In addition adsorbed methoxy, which presents a similar isotopic exchange kinetic than that of final products, could rather be an effective intermediate in methanol photooxidation.

However, even after a complete replacement of ¹³CH₃OH by ¹²CH₃OH in the gas phase (after t = 8 min, Figure S-6), traces of ¹²CO₂ could still be observed at t = 360 min, due to the slow decomposition of unlabeled surface formates. Two reaction pathways thus exist on the surface for the photocatalytic oxidation of methanol: a fast (and major) one, and a side-path, via the slow decomposition of surface formates. The fast reaction could go via some of the formates (could be the formates formed on the surface exposed directly to the light) or via surface carbonates, but no carbonate bands were detected. A slower rate for the isotopic exchange of surface formates was observed on TiO₂-L (crossing point at t >75 min vs. 18 min for TiO₂-P25). Switching to pure air, with zero methanol concentration, under UV irradiation, does not change the rate for formates removal from the surface. In addition, persistent IR bands were detected on the photocatalysts after isotopic exchange, due to stable formates formed on the surface after irradiation (in agreement with the observed influence of temperature).

Infrared spectra for TiOH groups on the surface during the photocatalytic process give information on the possible sites for the formation of weakly or not active formate species (Figure 10). The evolution of the IR spectra of TiO₂ in real time is presented in Figure S-7. Methanol adsorption led to the perturbation of surface TiOH groups and to the total disappearing of the IR bands at 3720 cm⁻¹ and 3690 cm⁻¹ assigned to the vibration bands of Ti(III)-OH and Ti(IV)-OH, respectively (Figure S-4). After irradiation, the Ti(IV)OH band was recovered while the Ti(III)OH band remained perturbed (Figure S-8). Figure 10B shows the linear relationship between the IR-bands of surface formate species and that of Ti(III)OH. This shows the role of TiOH functions in the stabilization of the formate on the photocatalyst surface. The higher band intensity for formates on TiO₂-L is thus due to a larger amount of TiOH sites on the surface of the solid. It should be noted that the higher absorption in the

visible for TiO₂-L is linked to the presence of oxygen vacancies and/or of Ti(III)-OH, resulting in an absorbance red-shift (Table 1).

Conclusion

The new *operando*-IR technique presented here shows high performance to highlight the activity of the photocatalyst, the selectivity of the reaction and the role of the surface species in the reaction mechanism. However, in situ identification of the species formed on the photocatalyst surface is not enough to determine their role in the reaction. We used the new technique to study the activity and selectivity of a new photocatalyst (TiO₂-L), with methanol photooxidation as model reaction for air purification from VOCs. TiO₂-P25 (Evonik-Degussa) was used as reference under the same reaction conditions. TiO₂-L presents a higher activity at low methanol concentration and higher selectivity at high methanol concentration compared to TiO₂-P25. The TOF of the reaction were calculated using a theoretical number of active site in TiO₂ anatase. It is 2 to 3 times lower in the case of TiO₂-L than for TiO₂-P25. This was assigned to an overestimation of the number of active sites in TiO₂-L and showed that the real number is lower than estimated. A similar methanol conversion rate (ml g_{TiO₂}⁻¹ min⁻¹) was found for both photocatalysts. The photooxidation activity and CO₂-selectivity of TiO₂ increase with temperature. Formate species are formed and adsorbed in higher amounts on TiO₂-L than on TiO₂-P25. A 40 cm⁻¹ shift could be also observed between IR spectra of TiO₂-P25 and TiO₂-L surfaces. SSITKA experiments allowed establishing relationships between surface species and final products. Formates formed on TiO₂-L are more stable than on TiO₂-P25. Most of formates observed by IR are spectator species. A relationship between the formation of formate and the disappearing of Ti(III)-OH was also observed, showing the role of defects and TiOH sites in the stabilization of low active formate on the surface. Isosbestic points between methoxy and final products were observed on both photocatalysts, suggesting methoxy as intermediates in methanol photooxidation. *Operando* IR is thus demonstrated as an important technique in photocatalysis, unveiling more information than other sometimes more expensive techniques. In the future, *operando* IR will be coupled with SSITKA using different methanol isotopes (CH₃¹⁸OH and CD₃OH) in order to determine the real intermediates and global mechanism in methanol photooxidation.

Tables.**Table 1.** Characteristic of TiO₂-L and TiO₂-P25 photocatalysts used in this work.

Photocatalyst	Crystallinity	Morphology	S _{BET} (m ² /g)	V _{meso} (cm ³ /g)	λ (nm)
TiO ₂ -L	Anatase (>95%)	Tubular macrofibers	90	0.14	<416
TiO ₂ -P25	Anatase (80%), Rutile (20%)	Agglomerated powders	55	--	<405

S_{BET}: BET surface; V_{meso}: mesoporous volume; λ: wave lengths of the photocatalyst absorbance.

Figures caption

Figure 1: influence of methanol concentration on methanol conversion and CO₂-selectivity for methanol photooxidation reaction using TiO₂-L (square) and TiO₂-P25 (circle) photocatalysts. (20% O₂/Ar vol.%; flow = 25 cm³/min; RT; I₀₍₃₆₆₎~10 mW/cm²; λ = 366 nm).

Figure 2: Original IR spectra of the gas phase during the photocatalytic reaction at RT, at different methanol concentrations. “a” corresponds to the IR spectrum of 1000 ppm of methanol before photooxidation.

Figure 3: Influence of methanol concentration on turnover frequency (TOF; close symbol) and on methanol conversion rate (in ml per gram of photocatalyst per minutes; open symbol) for the methanol photooxidation reaction using TiO₂-P25 (square) and TiO₂-L (circle) as photocatalysts. (20% O₂/Ar vol.%; flow=25 cm³/min; RT; I₀₍₃₆₆₎~10 mW/cm²; λ =366 nm).

Figure 4: IR spectra of TiO₂-L (A) and TiO₂-P25 (B) before (a) and after (b) 60 minutes of UV irradiation . (1200ppm of methanol in synthetic air; flow=25 cm³/min; RT; I₀₍₃₆₆₎~10 mW/cm²; λ =366 nm)

Figure 5: IR spectra of TiO₂-L (A) and TiO₂-P25 (B) after ~1h of methanol photooxidation at different methanol concentrations (Subtraction results from IR spectra recorded in the dark).

Figure 6: A) Evolution of the gas phase IR spectra vs reactor temperature for the methanol photooxidation reaction using TiO₂-L as photocatalyst. B) Evolution of methanol conversion (calculated using the IR band at 1090-950 cm⁻¹) and the IR band areas of CO₂ (2395-2182 cm⁻¹) and carbonyl species (R₂C=O; 1810-1717 cm⁻¹) at different temperatures. ([MeOH] = 1200ppm; I₀₍₃₆₆₎~10mW/cm²; λ=366nm; flow= 25 cm³/min; heating rate = 1°C/min and stabilization for ~1 h/temperature step).

Figure 7: A) Evolution of the IR band area of formate species at 1605cm⁻¹ and their derivative versus the temperature (d(IR band area)/dT) using TiO₂-L as photocatalyst. Figure (B) corresponds to the original IR spectra of TiO₂-L surface at different temperatures of methanol photooxidation.

Figure 8: IR spectra of TiO₂-P25 (A) and of the reaction gas phase (B) during a SSITKA experiment for which an initial flow of 1200 ppm of ¹²CH₃OH, 20% of oxygen diluted in Ar (total flow = 25 cm³ min⁻¹) was switched to a similar but labeled (¹³CH₃OH) flow (the spectrum recorded at t=0 was used as background). Figures (AII) and (BII) correspond to the original IR spectra of TiO₂-P25 and of the reaction gas phase, respectively, during the SSITKA experiment at t= 0 and 120 min.

Figure 9: Evolution of the IR band intensities for adsorbed species on TiO₂-P25 (A) and for final products detected in the gas phase (B) vs. irradiation time.

Figure 10: (A) Evolution of the IR band of Ti(III)OH at 3690 cm⁻¹ and of formate species at 1602 cm⁻¹ during methanol photooxidation. (B) Evolution of the formate species IR-band vs Ti(III)OH IR-band during methanol photooxidation.

Figures.

Figure 1

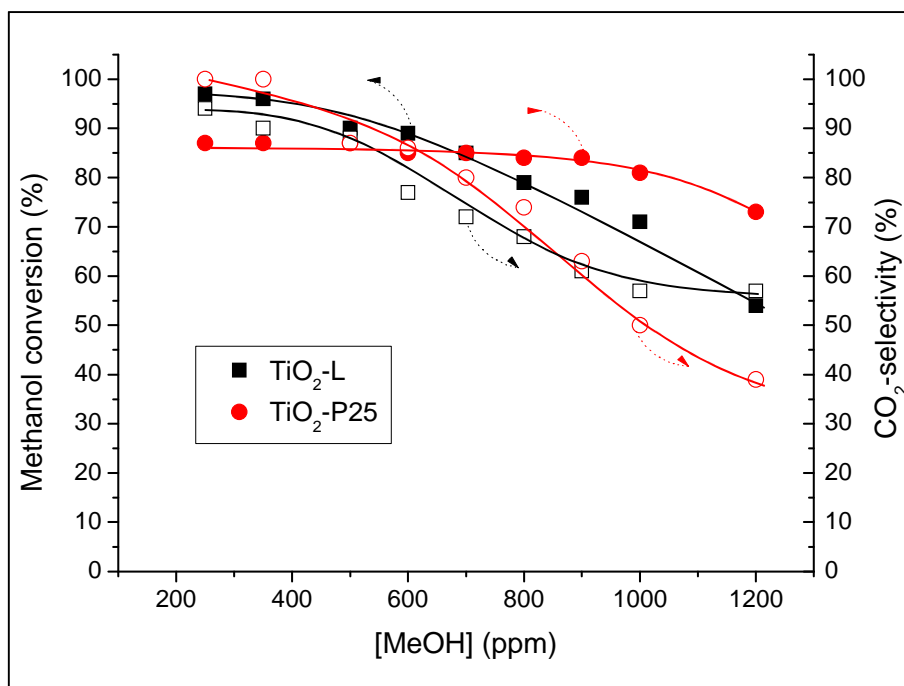


Figure 2

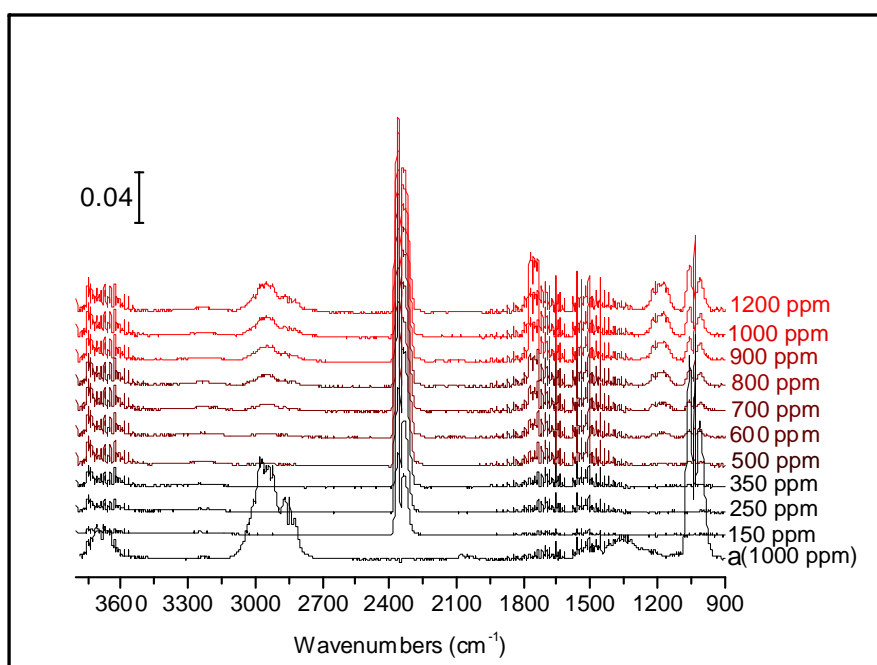


Figure 3

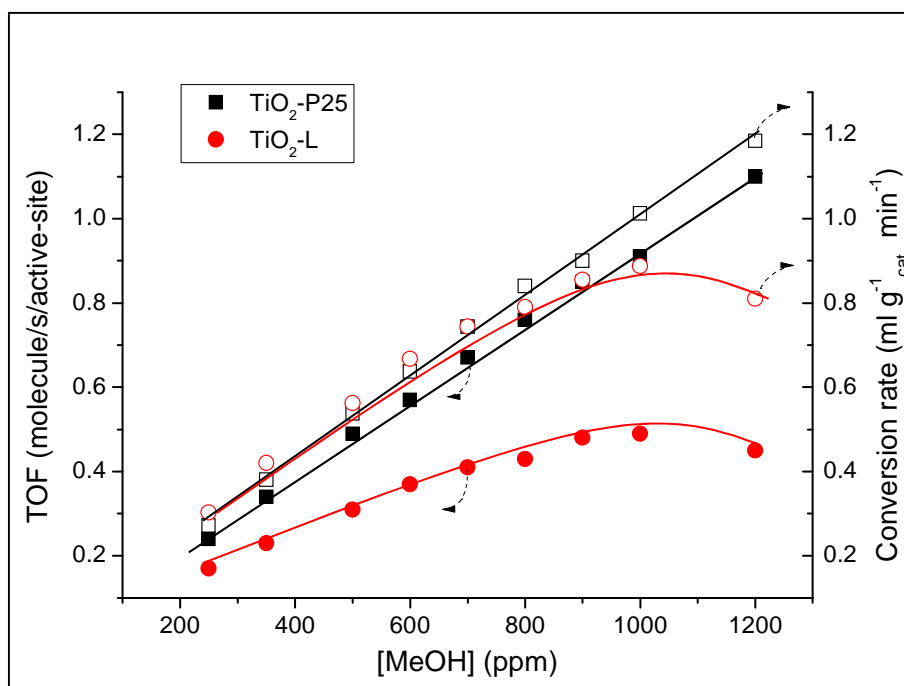


Figure 4

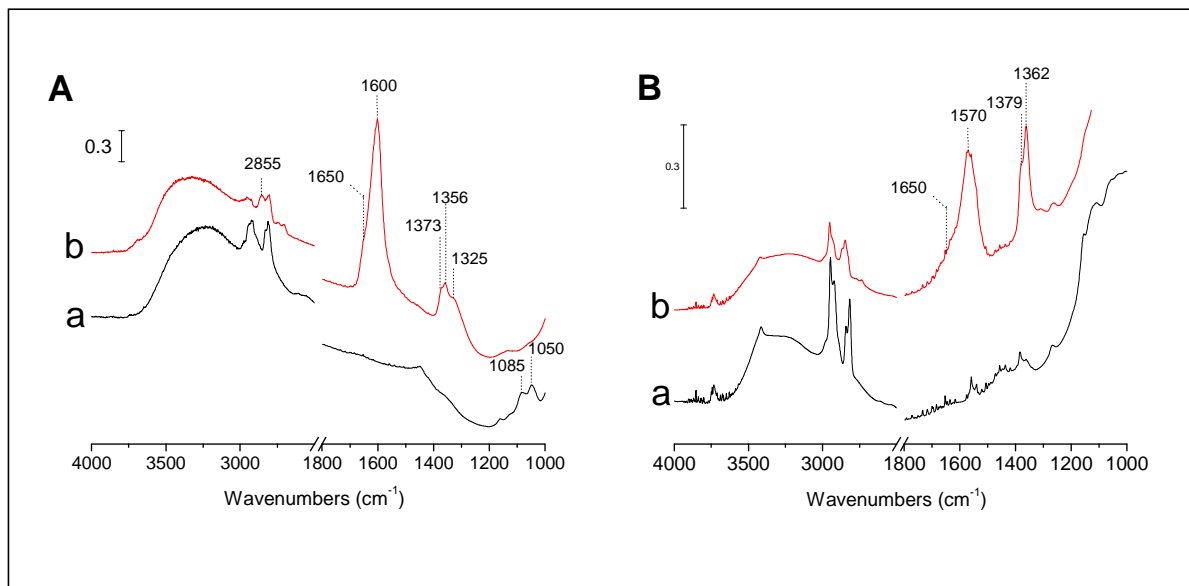


Figure 5

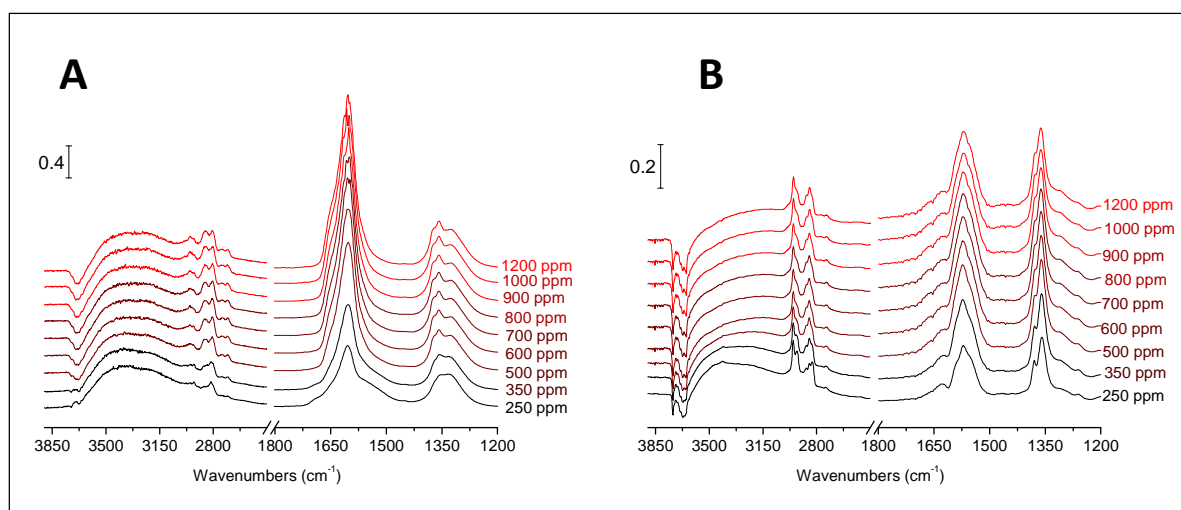


Figure 6

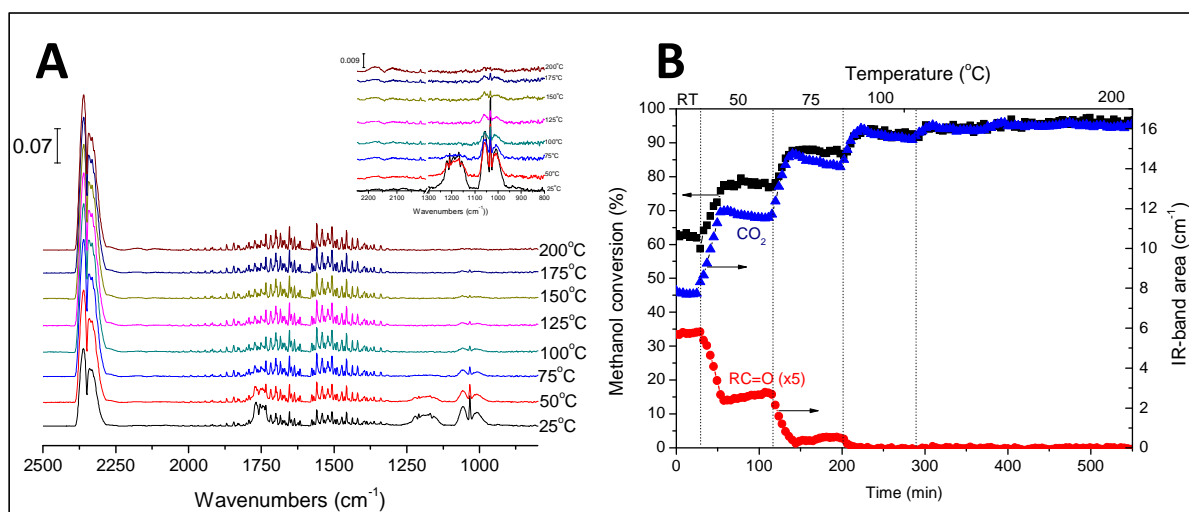


Figure 7

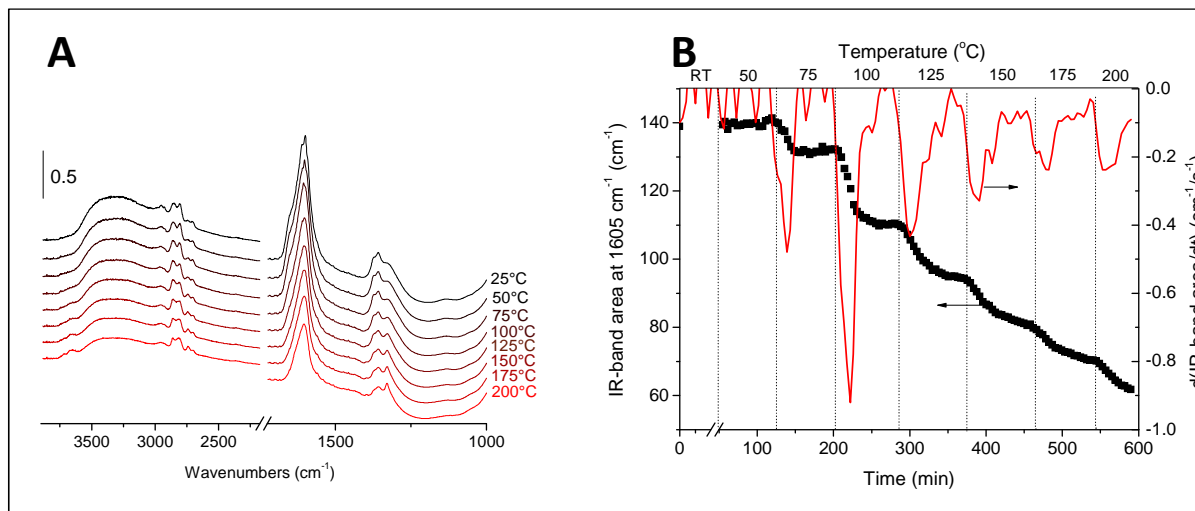


Figure 8

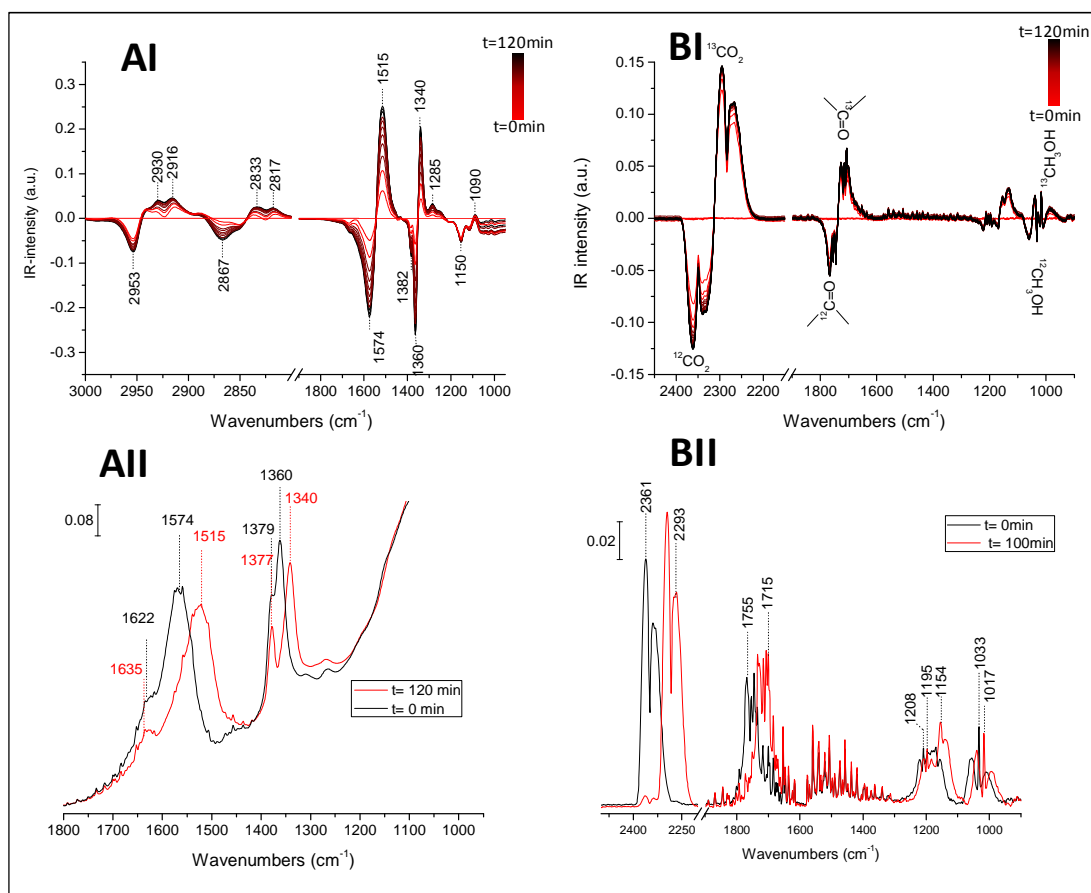


Figure 9.

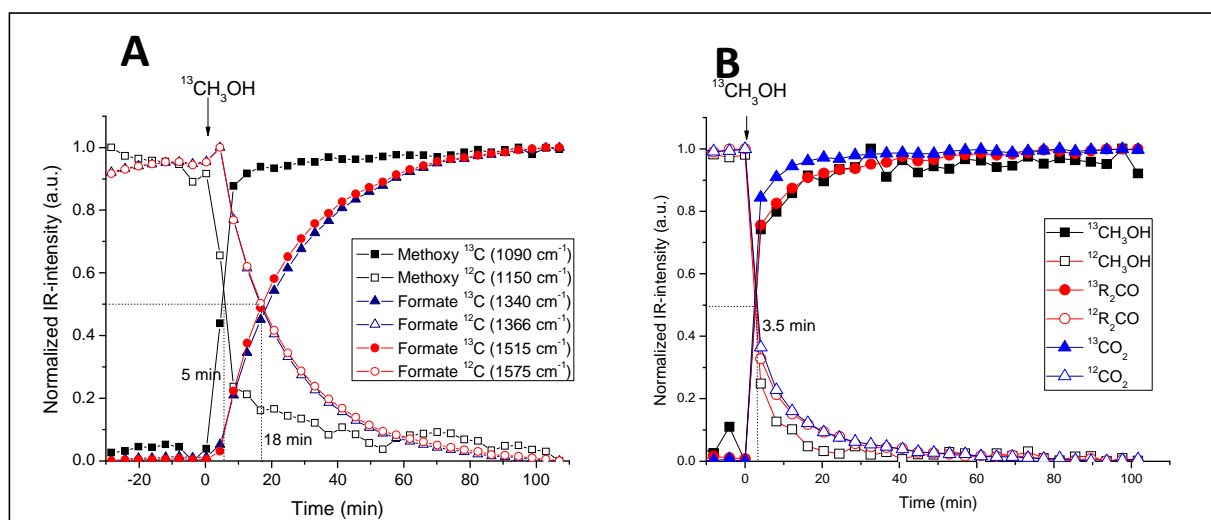
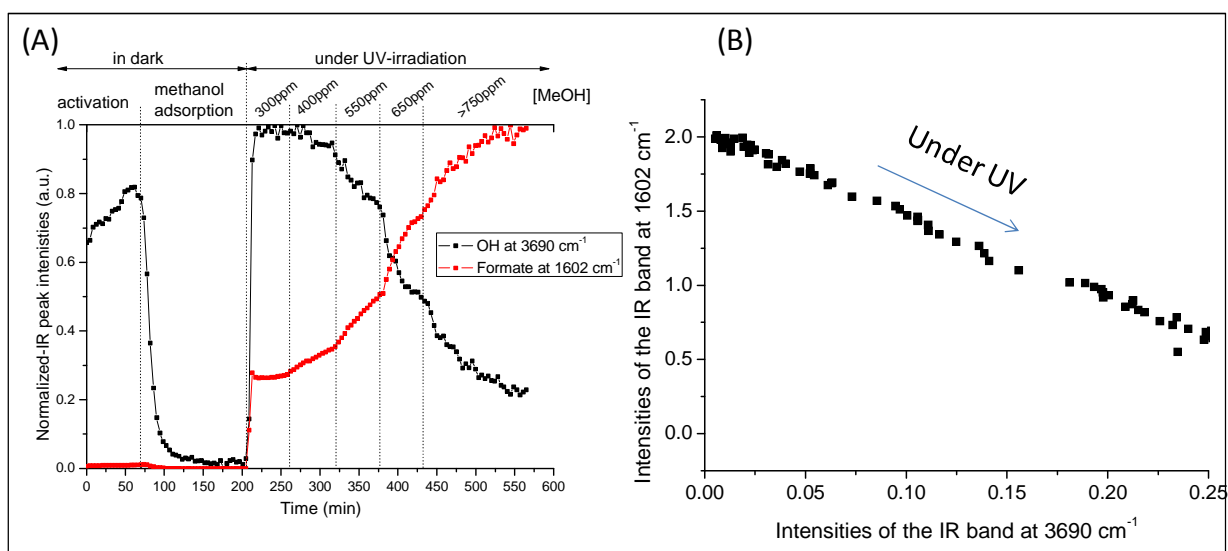
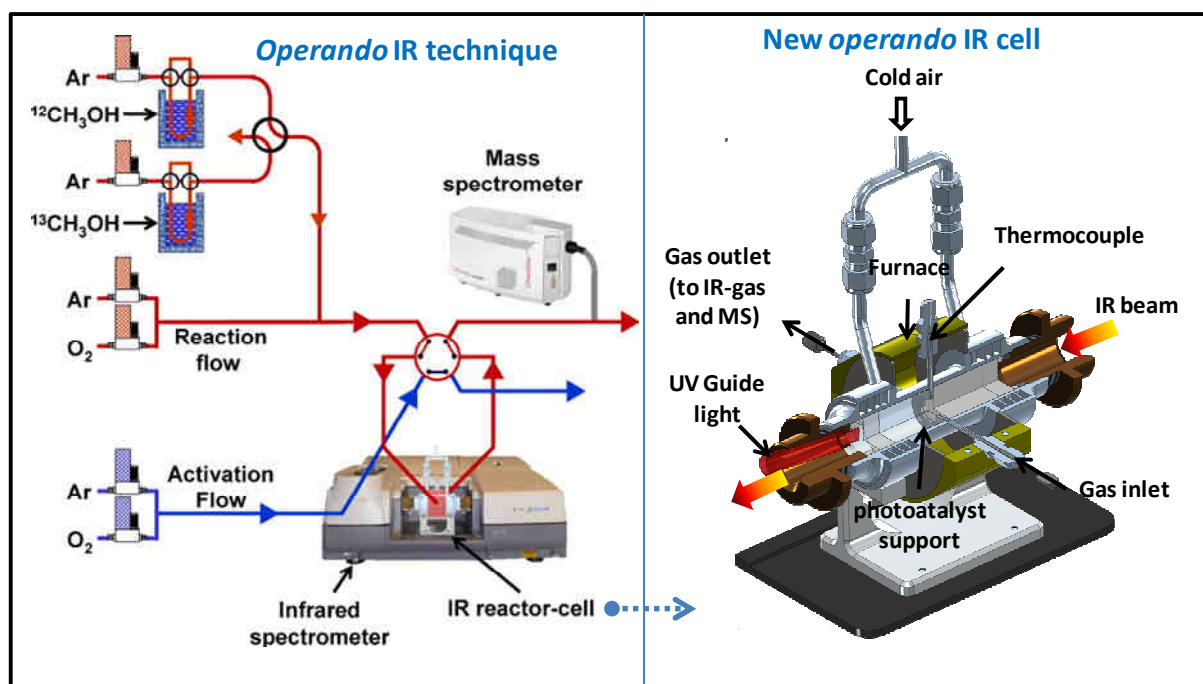


Figure 10.



Supplementary information



Scheme S1. Scheme of the SSITKA equipment used and of the sandwich reactor-IR cell modified for UV catalysis study.

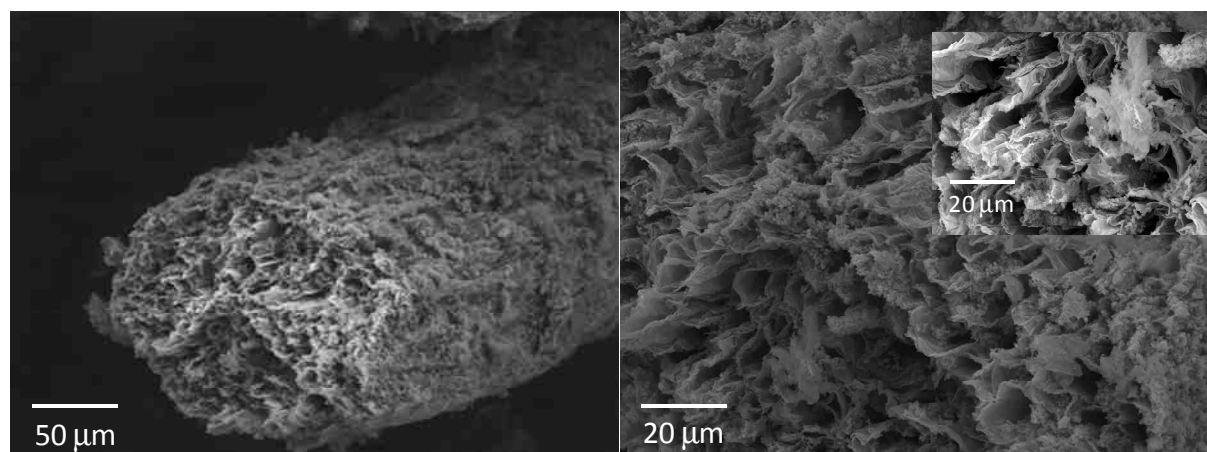


Figure S-1. SEM micrographs of self-supporting (calcined) TiO_2 replica of Luffa sponge (TiO₂-L).

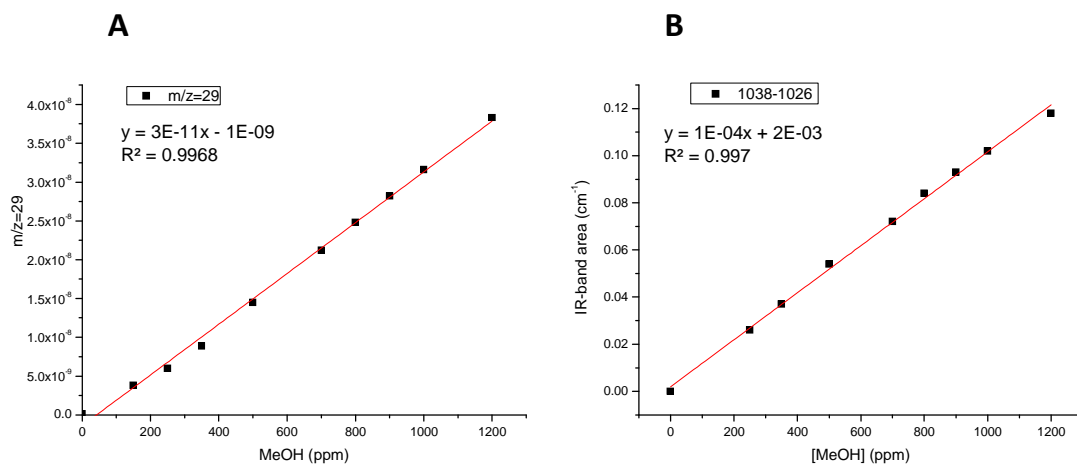


Figure S-2. Methanol calibration curve using the MeOH-MS signal (at $m/z=29$) (A) and characteristic MeOH-IR band area (at $1038-1026\text{ cm}^{-1}$) (B).

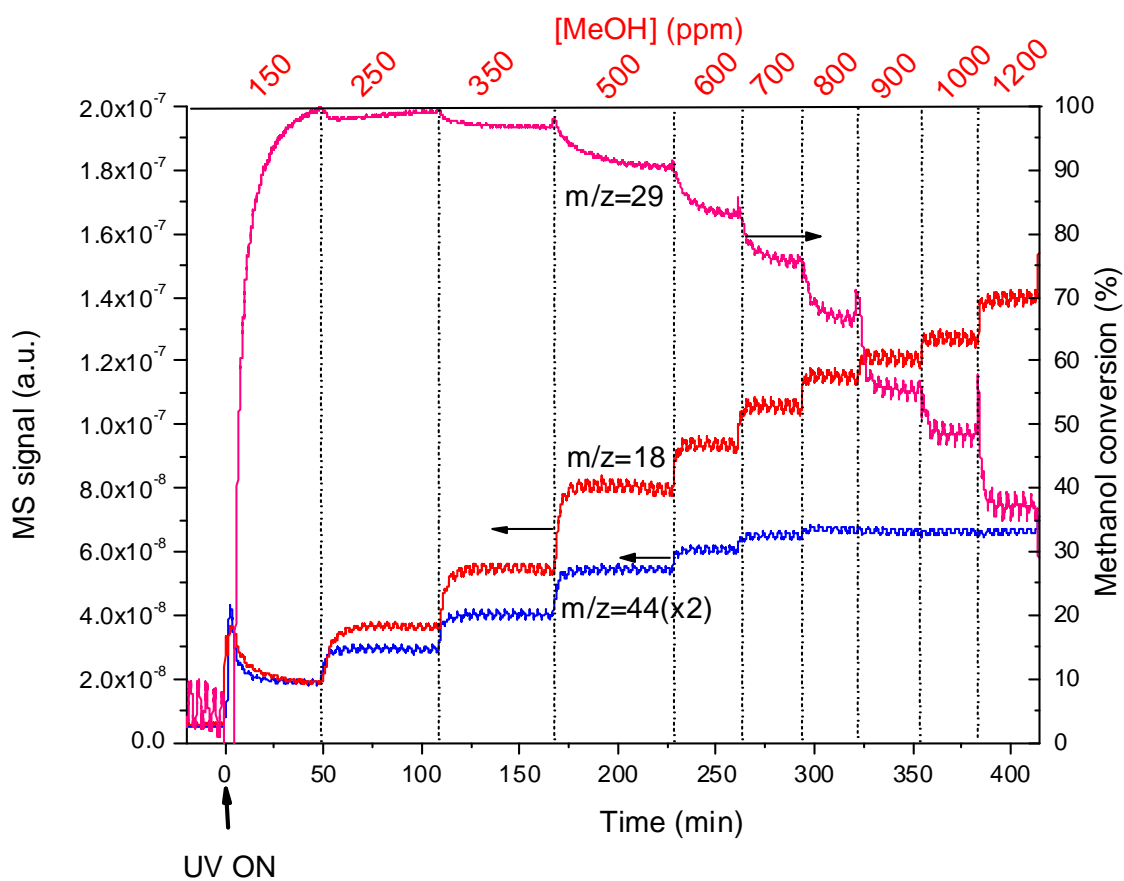


Figure S-3. Evolution of the methanol conversion (calculated using $m/z=29$ MS signal), the MS signal of CO_2 ($m/z=44$) and of H_2O ($m/z=18$) versus different methanol concentrations and irradiation time.

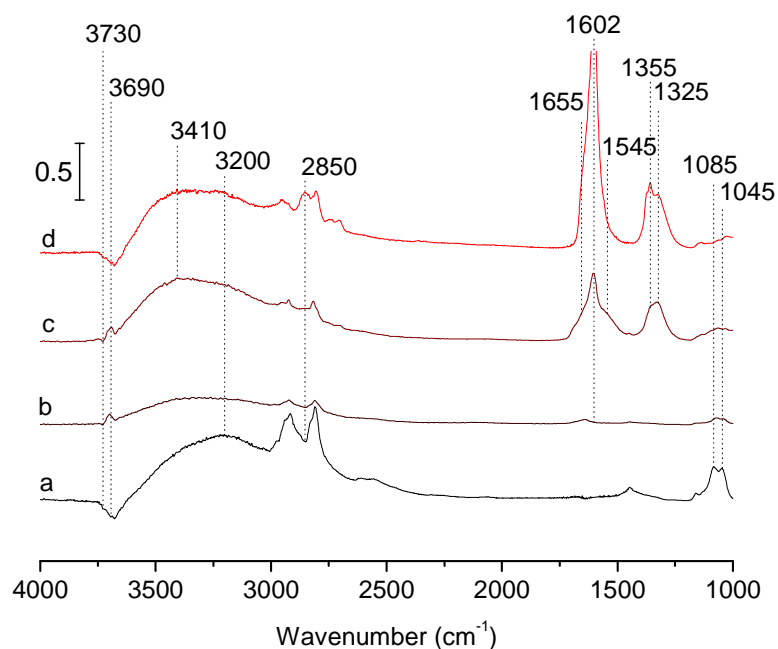


Figure S-4. IR spectra of $\text{TiO}_2\text{-L}$ before (a) and during methanol photooxidation at $t=0$ min (b) 30 min (c) and 360 min (d) (t =irradiation time). (Subtracted results from IR spectrum of $\text{TiO}_2\text{-L}$ after activation at 500°C , taken as the reference).

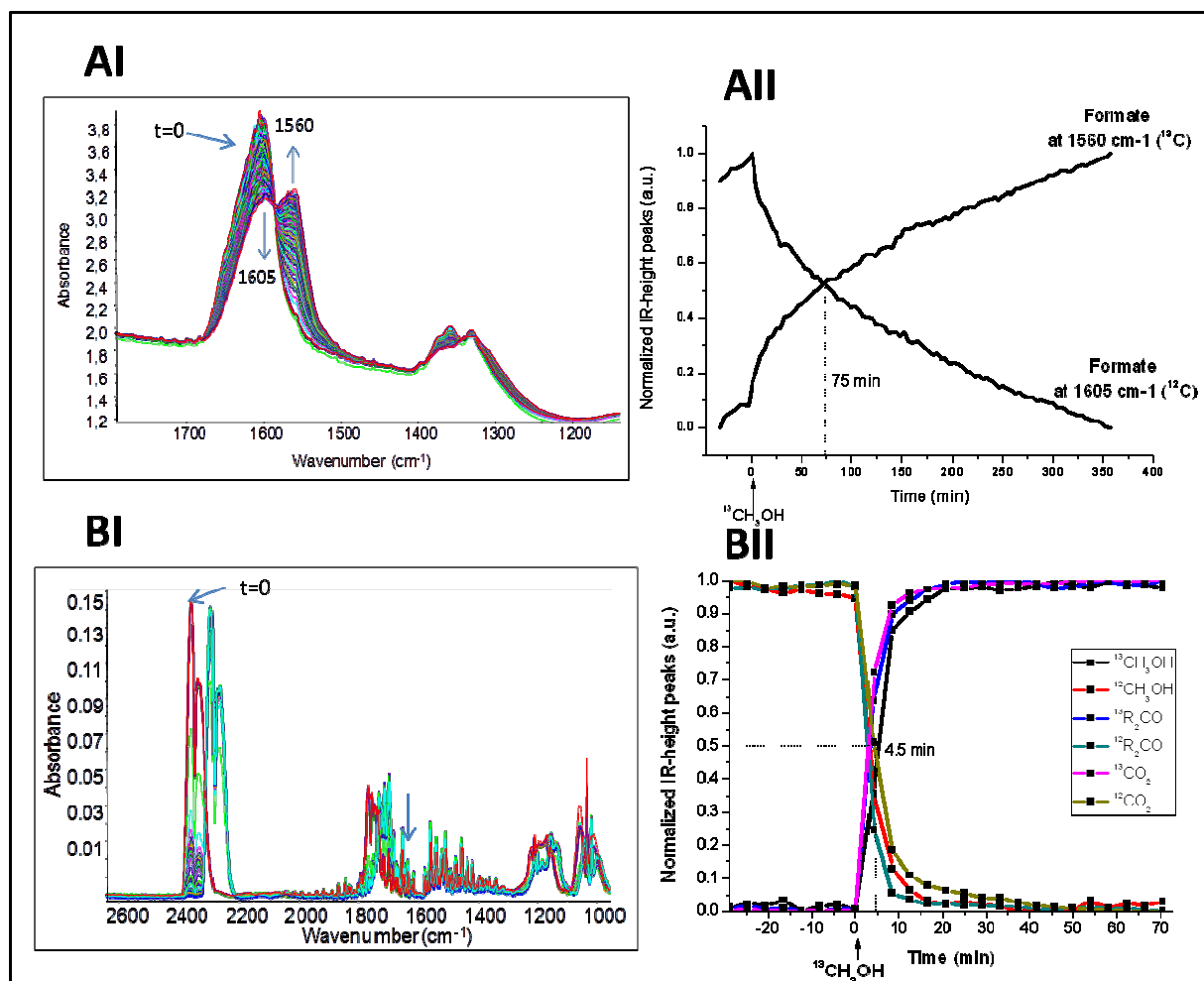


Figure S-5. IR spectra of $\text{TiO}_2\text{-L}$ (A) and of the reaction gas phase (B) recorded at 25°C during a SSITKA experiment for which an initial flow made of 1200 ppm of $^{12}\text{CH}_3\text{OH}$, 20% of oxygen diluted in Ar (total flow = $25 \text{ cm}^3 \text{ min}^{-1}$) was switched to a similar labeled ($^{13}\text{CH}_3\text{OH}$) flow (Spectra subtracted from the spectrum recorded at $t = 0$, which corresponds to the switch moment of $^{12}\text{CH}_3\text{OH}/^{13}\text{CH}_3\text{OH}$). Figures (AII) and (BII) corresponds to the evolution of the IR band intensities of the species adsorbed on the photocatalyst surface and to those of final products detected in the gas phase, respectively, vs. irradiation time.

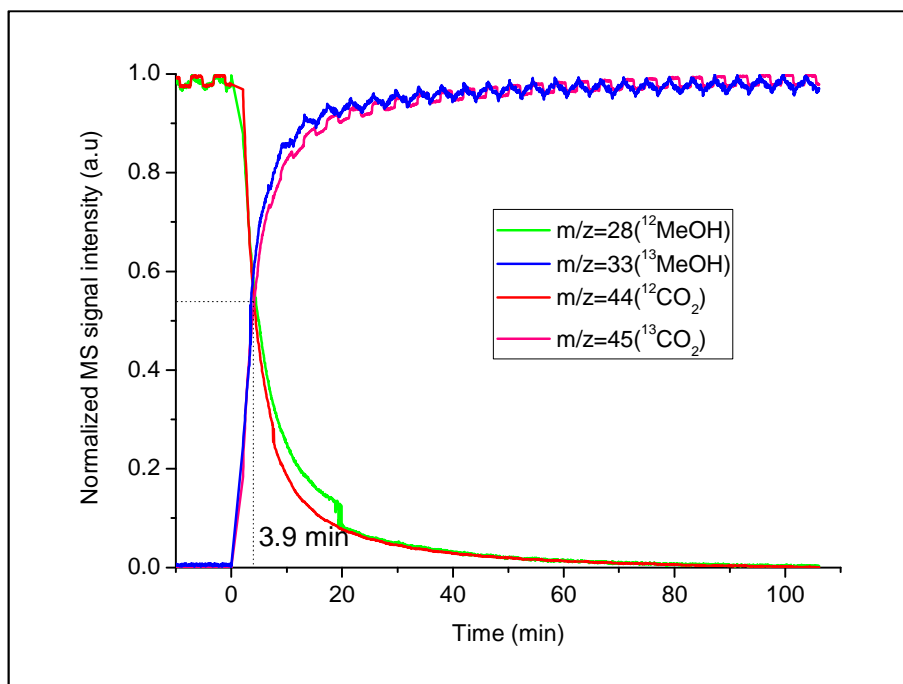


Figure S-6. Evolution of the normalized MS signal intensities of $^{12}\text{CH}_3\text{OH}$ ($m/z=28$), $^{13}\text{CH}_3\text{OH}$ ($m/z=33$), $^{12}\text{CO}_2$ ($m/z=44$), and $^{13}\text{CO}_2$ ($m/z=45$) during a SSITKA experiment of methanol photooxidation.(same conditions as mentioned in Figure 9).

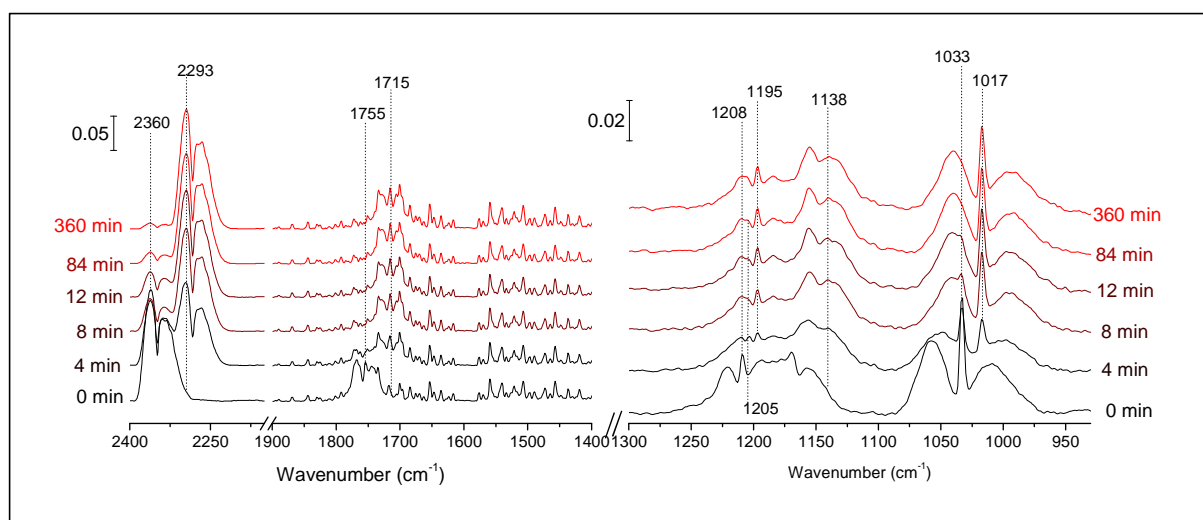


Figure S-7: IR spectra of the methanol photooxidation gas phase recorded at different times of SSITKA experiment.

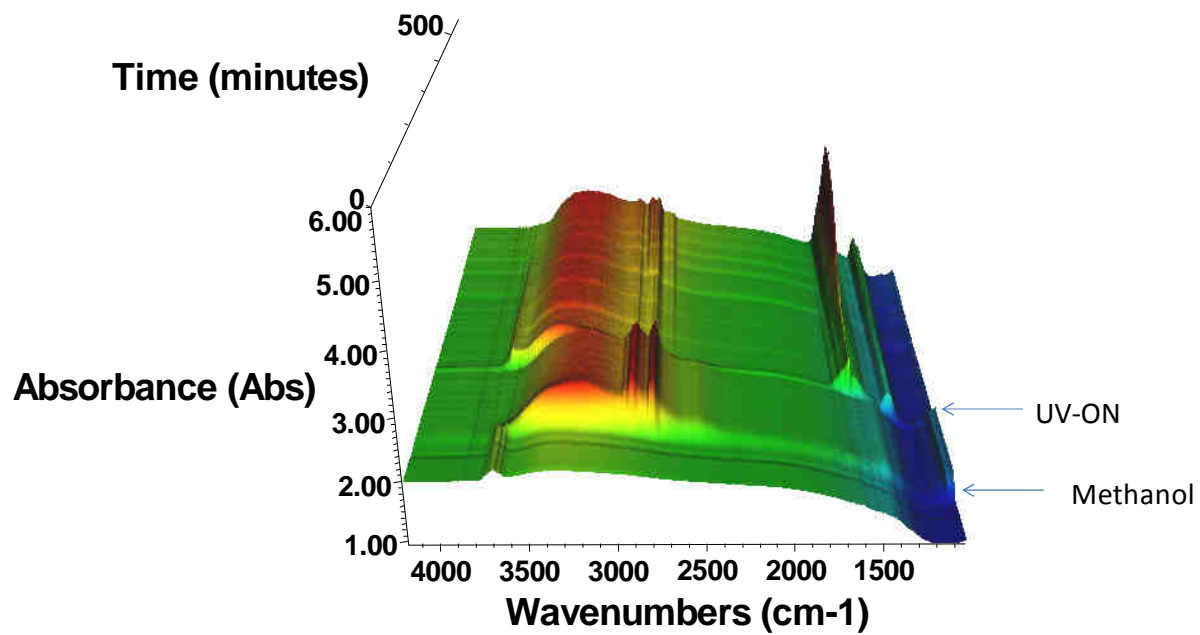


Figure S-8: Evolution of the IR spectra of TiO₂-L during methanol photooxidation.

Table S-1. Data obtained in the photooxidation of different methanol concentrations using TiO₂-P25 and TiO₂-L photocatalysts.

[MeOH] (ppm)	TiO ₂ -P25				TiO ₂ -L			
	Conv. (%)	CO ₂ - selectivity (%)	TOF (molecules/s/active site)	V _{MeOH} (ml g ⁻¹ cat min ⁻¹)	Conv. (%)	CO ₂ - selectivity (%)	TOF (molecules/s/active site)	V _{MeOH} (ml g ⁻¹ cat min ⁻¹)
250	87	99	0.24	0.27	97	95	0.17	0.30
350	87	99	0.34	0.38	96	90	0.23	0.42
500	86	90	0.49	0.54	90	88	0.31	0.56
600	85	86	0.57	0.64	89	77	0.37	0.67
700	85	80	0.67	0.74	85	72	0.41	0.74
800	84	74	0.76	0.84	79	68	0.43	0.79
900	80	63	0.85	0.9	76	60	0.48	0.85
1000	81	50	0.91	1.0	71	57	0.49	0.89
1200	73	39	0.84	1.1	54	57	0.45	0.81

References

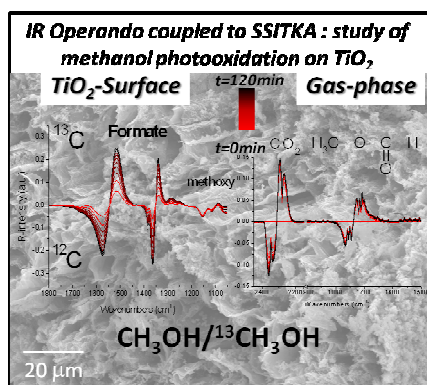
- ¹ Athanasekou, C.P. ; Romanos, G.E.; Katsaros, F.K. ; Kordatos, K.V. ; Likodimos, Falaras, P. *J. Membr. Sci.* **2012**, 392,192-203.
- ² Maroga Mboulaa, V. ; Hequeta, V. ; Grub, Y. ; Colinb, R. ; Andresa, Y.; *J. Hazard. Mat.* **2012**, 209, 355-364.
- ³ Wilsonb, D. ; Wangb, W. ; Lopesa, R. J.G. *App. Cat. B: Env.* **2012**, 123, 273-281.
- ⁴ Konstantinou, I.K. ; Albanis, T. A. *App. Catal. B: Env.* **2004**, 49, 1-14.
- ⁵ Gogate, P.R ; Pandit, A. B *Adv. Env. Res.* **2004**, 8, 501-551.
- ⁶ Galindo, C. ; Jacques, P. ; Kalt, A. *J. Photochem. Photobiol. A: Chem.* **2000**, 130, 35-47.
- ⁷ Fujishima, A. ; Zhangb, X. ; Tryk, D. A. *Surf. Sci. Rep.* **2008**, 63, 515-582.
- ⁸ Fujishima, A. ; Zhangb, X. *C. R. Chimie* **2006**, 9, 750-760.
- ⁹ Ganesh, V. A.; Kumar Raut, H.; Nair, A. S.; Ramakrishna, S. *J. Mater. Chem.* **2011**, 21, 16304-16322.
- ¹⁰ Web of knowledge, Thomson Reuters, <http://wokinfo.com>, **2013**.
- ¹¹ Scifinder® site, CAS, <https://scifinder.cas.org>, **2013**.
- ¹² El-Roz, M. ; Kus, M. ; Cool, P. ; Thibault-Starzyk, F. *J. Phys. Chem. C* **2012**, 116, 13252-13263.
- ¹³ El-Roz, M.; Bazin, P.; Thibault-Starzyk, F. *Catal. Today*, **2013**, 205, 111-119.
- ¹⁴ Rousseau, S. ; Marie, O. ; Bazin, P. ; Daturi, M. ; Verdier, S. ; Harlé, V. ; *J. Am. Chem. Soc.*, **2010**, 132, 10832-10841.
- ¹⁵ Sun, S.; Ding, J.; Bao, J.; Gao, C.; Qi, Z.; Li, C. *Catal Lett.* **2010**, 137, 239-246.
- ¹⁶ Panayotov, D. A.; Burrows, S. P.; Morris, J. R. *J.Phys.Chem. C* **2012**, 116, 6623-6635.
- ¹⁷ Bazin, P. ; Thomas, S. ; Marie, O. ; Daturi, M. *Catal. Today* **2012**, 182, 3-11.
- ¹⁸ M., El-Roz; Haidar, Z.; Al-Lakiss, L.; Toufaily, J.; Thibault-Starzyk, F. *RCS Advances*, **2013**, 3, 3438-3445.
- ¹⁹ Lesage, T.; Verrier, C.; Bazin, P.; Saussey, J.; Daturi, M. *Phys. Chem. Chem. Phys.* **2003**, 5, 4435-4440.

-
- ²⁰ Malpartida, I. ; Ivanova, E. ; Mihaylov, M. ; Hadjiivanov, K. ; Blasin-Aubé, V. ; Marie, O. ; Daturi, M. *Catal. Today* **2010**, *149*, 295-303.
- ²¹ Wuttke, S.; Bazin, P.; Vimont, A.; Serre, C.; Seo, Y.-K.; Hwang, Y. K.; Chang, J.-S.; Férey, G.; Daturi, M. *Chem. Eur. J.* **2012**, *18*, 11959-11967.
- ²² Herrmann, J.-M. *J. Photochem. Photobio. A: Chem.* **2010**, *216*, 85-9.
- ²³ Boudart, M. ; Djéga-Mariadassou, G. *Cinétique des réactions en catalyse hétérogène*, Masson, Paris, **1982**.
- ²⁴ Parmon, V. ; Emeline, A.V. ; Serpone, N. *Int. J. Photoenergy*, **2002**, *4*, 91-131.
- ²⁵ Braslavsky, S. E. Braun, A. M. ; Cassano, A. E. ; Emeline, A.V.; Litter, M. I. ; Palmisano, L. ; Parmon, V. N. ; Serpone, N. *Pure Appl. Chem.* **2011**, *83*, 931-1014.
- ²⁶ Boehm, H.P. *Adv. Catal.* **1966**, *16*, 179-274.
- ²⁷ Chuang, C.C.; Wu, W.C.; Huang, M.C.; Huang, I.C.; Lin, J.L. *J. Catal.* **1999**, *185*, 423-434.
- ²⁸ Popova, G.Y.; Andrushkevich, T.V.; Chesalov, Y.A. ; Stoyanov, E.S. *Kinetics and Catalysis*, **2000**, *41*, 805–811.
- ²⁹ Hernandez-Alonso, M.; Tejedor-Tejedor, I.; Coronado, J. M.; Anderson, M. A. *Appl. Catal. B: Environ.* **2011**, *101*, 283-293.
- ³⁰ Arana, J.; Dona-Rodriguez, J.M.; Cabo, C. G. i; Gonzalez-Diaz, O.; Herrera-Melian, J.A. ; Perez-pena, J. *Appl. Catal. B: Environ.* **2004**, *53*, 221-232.
- ³¹ Kominami, H. ; Sugahara, H.; Hashimoto, K. *Catal. Commun.* **2010**, *11*, 426-429.
- ³² Coronado, J. M. ; Kataoka, S.; Tejedor-Tejedor, I.; Anderson, M. A. *J. catal.* **2003**, *219*, 219-230.
- ³³ ven der Meulen, T.; Mattson, A.; Osterlund, L. *J. Catal.* **2007**, *251*, 131-144.
- ³⁴ Guzman, F. ; Chuang, S. S.C. *J. Am. Chem. Soc.* **2010**, *132*, 1502-1503.
- ³⁵ Bazin, P. ; Thomas, S. ; Marie, O. ; Daturi, M. *Catal. Today* **2012**, *182*, 3-11.
- ³⁶ Efstathiou, A.M.; Verykios, X.E. *Appl. Catal. A: Gen.* **1997**, *151*, 109-166.
- ³⁷ Olympiou, G.G.; Kalamaras, C.M.; Zeinalipour-Yazdi, C.D.; Efstathiou, A.M. *Catal. Today*, **2007**, *127*, 304-318.
- ³⁸ Meunier, F.C.; Reid, D.; Goguet, A.; Shekhtman, S.; Hardacre, C.; Burch, R.; Deng, W.;

Flytzani-Stephanopoulos, M. J. *Catal.* **2007**, *247*, 277-287.

³⁹ Wang, J.; Kispersky, V. F.; Delgass, W. N.; Ribeiro, F. H. *J. Catal.* **2012**, *289*, 171-178.

TOC



Evolution of IR spectra of TiO₂ surface and reaction gas phase after CH₃OH/¹³CH₃OH isotopic exchange during methanol photooxidation (t=0 correspond to exchange moment).